Direct Detection with Phase Recovery in Optical Communications

Research internship from 5. 2023 to 11. 2023

Diego Alejandro Figueroa Del Castillo | 16. January 2024

Table of contents I

Table of contents II

Introduction

Motivation

Square-law detection, also known as Direct detection (DD), is a detection scheme that measures the square magnitude of a complex waveform.

- Nonlinear detection
- Used specifically in short-haul systems (up to $50\,\mathrm{km}$)

Why is Direct Detection relevant?

- The receiver hardware is simple
- Low-cost alternative compared to the coherent detection

Direct detection

Direct Detection is performed with a single photodiode that converts the optical signal into an electric signal.

$$I_p = R_d \cdot P_{\text{in}} \tag{1}$$

$$P_{\text{in}} \propto E_{\text{in}}^2 \tag{2}$$

The detection is affected by the shot and thermal noise.

$$I(t) = I_p + i_s(t) + i_{th}(t) \tag{3}$$

with $i_s(t) \sim \mathcal{N}(0, \sigma_s^2)$ and $i_{th}(t) \sim \mathcal{N}(0, \sigma_{th}^2)$, and

$$\sigma_s^2 = 2qI_pB \qquad \sigma_{th}^2 = \frac{4k_BT}{R_L}F_nB \tag{4}$$

Capacity under direct detection

Direct Detection can retrieve only the information about the magnitude of the signal, so it is reasonable to think that the capacity of this system should be reduced by a half.

Capacity loss

In Mecozzi and Shtaif 2018; Tasbihi and Kschischang 2020 it is shown that the spectra efficiency of a band-limited or time-limited system under Direct Detection is at most $1\,\mathrm{bit/s/Hz}$ less than the same system under coherent detection.

$$I_{\mathrm{CD}} - 1 \leq I_{\mathrm{DD}} \leq I_{\mathrm{CD}} \tag{5}$$

Basic principle of phase recovery

Given two complex numbers z_1 and z_2; from $|z_1|^2$, $|z_2|^2$ and $|z_1 + z_2|^2$ (an ISI term), it is possible to determine the phase difference between z_1 and z_2 up to a sign ambiguity.

$$\begin{aligned}
|z_1 + z_2|^2 &= (z_1 + z_2)(z_1 + z_2)^* \\
&= z_1 z_1^* + z_1 z_2^* + z_2 z_2^* + z_1^* z_2 \\
&= |z_1|^2 + |z_2|^2 + z_1 z_2^* + \left(z_1 z_2^*\right)^* \\
&= |z_1|^2 + |z_2|^2 + 2\text{Re}\{z_1 z_2^*\}
\end{aligned}$$

under the convention that $z_1 = a \cdot e^{j\alpha}$ and $z_2 = b \cdot e^{j\beta}$

$$|z_1 + z_2|^2 = |z_1|^2 + |z_2|^2 + 2|z_1||z_2| \cos(\alpha - \beta) \tag{6}$$

Basic principle of phase recovery

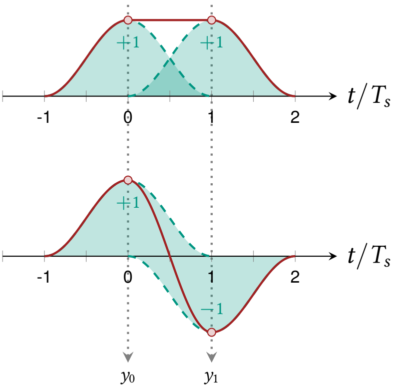

Figure 1: Coherent Detection

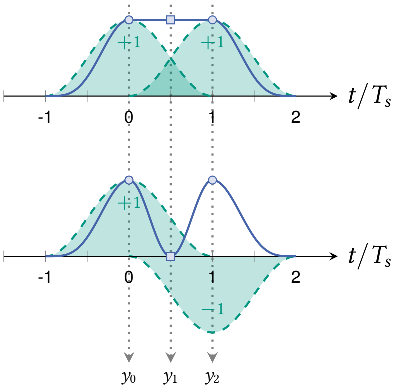

Figure 2: Direct detection

Tukey signaling

System model

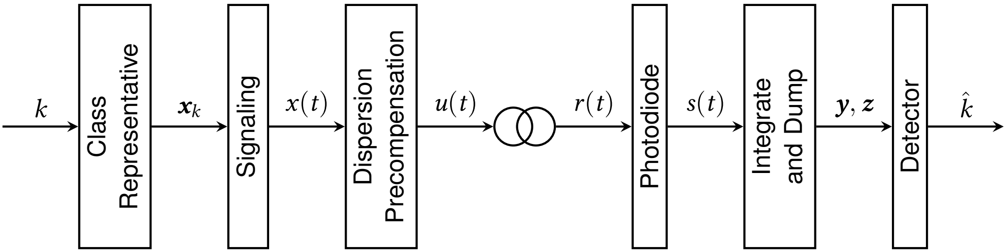

System model
Dispersion precompensation

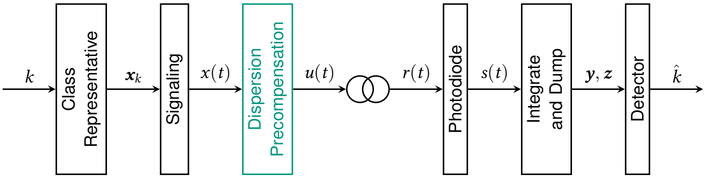

All-pass filter with a transfer function given by :

$$H(f) = e^{j2\beta_2 L\pi^2 f^2} \tag{7}$$

where β_2 is the group-velocity dispersion parameter and L is the fiber length .
The following relations between $x(t)$ and $u(t)$ are given:

$$u(t) = \mathcal{F}^{-1}\{X(f)H(f)\} \tag{8}$$

System model
Transmission medium

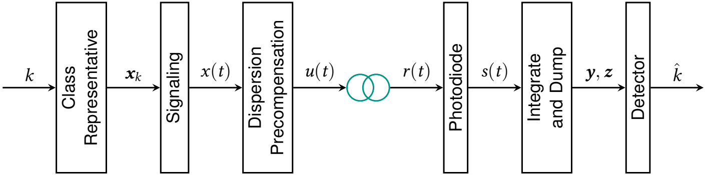

Since the optical fiber length is less than $10\,\text{km}$, we ignore all the transmission impairments, except for power loss and chromatic dispersion .

$$r(t) = \rho x(t) \tag{9}$$

where $0 < \rho \leq 1$ is the attenuation constant.

System model
Photodiode

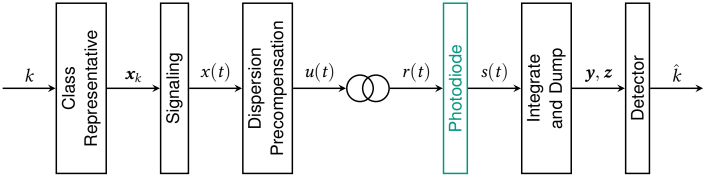

An avalanche photodiode is used for this system, and this diode is considered the only noise source. Both shoot and thermal noise are considered.

$$s(t) = \left|r(t)\right|^2 + \left|r(t)\right| n_{sh}(t) + n_{th}(t) \tag{10}$$

where $n_{sh}(t)$ and $n_{th}(t)$ are Gaussian distributed, and the variance of each noise is given by :

$$\sigma_{th}^2 = \frac{4k_B TB}{R_L} \qquad \sigma_{sh}^2 = 2qM_{\mathsf{APD}}^2 FR_{\mathsf{APD}} B \tag{11}$$

System model
Signaling

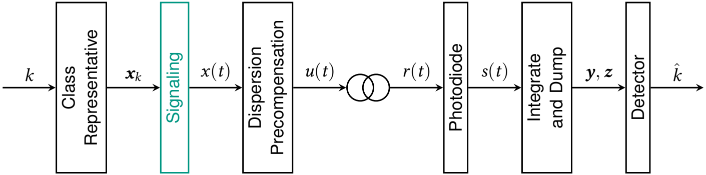

This block receives n complex numbers $x_0, \ldots, x_{n-1}$, which are the transmitted symbols, and produces a continuous time complex signal given by:

$$x(t) = \sum_{i=0}^{n-1} x_i w(t - iT) \tag{12}$$

where T is the inverse of the baud rate and $w(t)$ is a waveform.

System model
Waveform

The proposed waveform is the Tukey window, which is equivalent to the Fourier transform of a raised cosine but in the time domain. This waveform is given by:

$$w_\beta(t) = \begin{cases} \frac{2}{\sqrt{4-\beta}} & \text{if } |t| \leq \frac{1-\beta}{2} \\ \frac{1}{\sqrt{4-\beta}} \left(1 - \sin\left(\frac{\pi(2|t|-1)}{2\beta}\right)\right) & \text{if } \left||t| - \frac{1}{2}\right| \leq \frac{\beta}{2} \\ 0 & \text{otherwise} \end{cases} \tag{13}$$

$$W_\beta(f) = \begin{cases} \frac{\pi}{2\sqrt{4-\beta}} \cdot \text{sinc}\left(\frac{1}{2\beta}\right) & \text{if } f = \pm\frac{1}{2\beta} \\ \frac{2}{\sqrt{4-\beta}} \cdot \text{sinc}(f) \cdot \frac{\cos(\pi\beta f)}{1-(2\beta f)^2} & \text{otherwise} \end{cases} \tag{14}$$

System model
Waveform

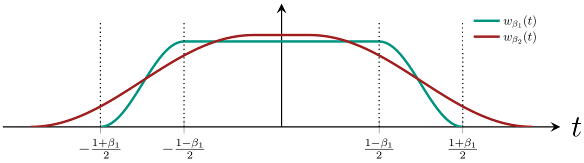

(a) Time domain

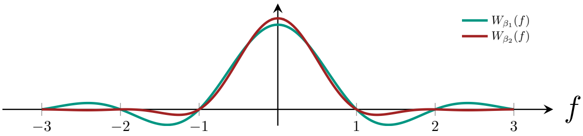

(b) Frequency domain

Figure 3: Tukey window for different β, $\beta_1 < \beta_2$. Based on .

System model
Waveform

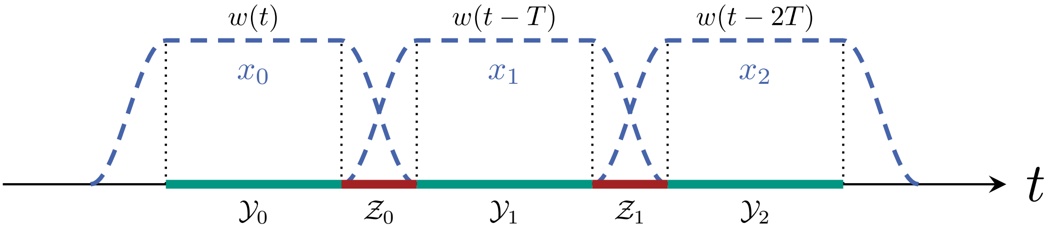

Figure 4: ISI-free and ISI-pressent intervals for $n = 3$. Based in .

System model
Integrate and dump

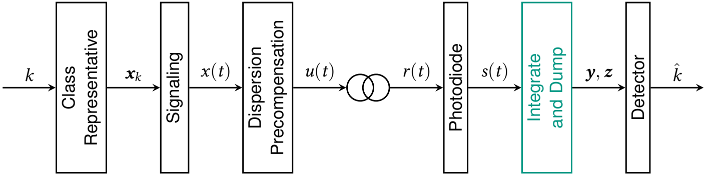

This block integrates the incoming signal $s(t)$ in the different intervals $\mathcal{Y}_i$ and $\mathcal{Z}_i$ to produce the real valued samples y_i and z_i given by:

$$y_i = \int_{\mathcal{Y}_i} s(t)dt \qquad i \in \{0, \ldots, n-1\} \tag{15}$$

$$z_i = \int_{\mathcal{Z}_i} s(t)dt \qquad i \in \{0, \ldots, n-2\} \tag{16}$$

System model
Integrate and dump

It can be shown that y_i is given by :

$$y_i = \alpha^2(1-\beta)T|x_i|^2 + \alpha|x_i|n_i + m_i \quad (17)$$

where $\alpha = 2/\sqrt{4-\beta}$, $n_i \sim \mathcal{N}(0, \sigma_{sh}^2(1-\beta)T)$ and $m_i \sim \mathcal{N}(0, \sigma_{th}^2(1-\beta)T)$.
And that z_i is given by :

$$z_i = \alpha^2\beta T\psi(x_i, x_{i+1}) + \alpha\sqrt{\psi(x_i, x_{i+1})}p_i + q_i \quad (18)$$

where $p_i \sim \mathcal{N}(0, \sigma_{sh}^2\beta T)$ and $q_i \sim \mathcal{N}(0, \sigma_{th}^2\beta T)$, and

$$\psi(ae^{j\alpha}, be^{j\beta}) = \frac{3}{8}\left(a^2 + b^2\right) + \frac{1}{4}ab\cos(\alpha-\beta) \quad (19)$$

System model
Class representative

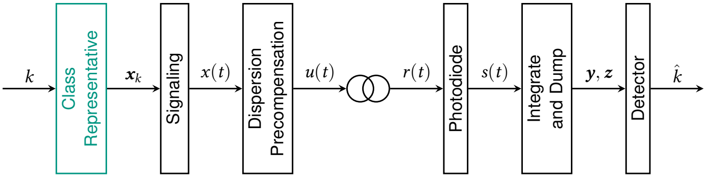

When transmitting symbol blocks (n consecutive symbols), it turns out that there are some ambiguities, which means that two different symbol blocks produce the same output of the system. Of course, we want to avoid this situation to achieve reliable communication. That is what the Class representative block does.

System model
Class representative

let define the function $\Upsilon : \mathbb{C}^n \to (\mathbb{R}^n, \mathbb{R}^{n-1})$ that maps a vector $\boldsymbol{x}$ at the input of the signaling block, to the output of the integrate and dump block, in the absence of noise. That means:

$$\Upsilon(\boldsymbol{x}) = (\boldsymbol{y}, \boldsymbol{z}) \tag{20}$$

where $\boldsymbol{x} \in \mathbb{C}^n$, $\boldsymbol{y} \in \mathbb{R}^n$, $\boldsymbol{z} \in \mathbb{R}^{n-1}$ and

$$y_i = \int_{\mathcal{Y}_i} \left|x(t)\right|^2 dt \qquad i \in \{0, \ldots, n-1\} \tag{21}$$

$$z_i = \int_{\mathcal{Z}_i} \left|x(t)\right|^2 dt \qquad i \in \{0, \ldots, n-2\} \tag{22}$$

Now we define an equivalence relation in $\mathbb{C}^n$, where two vectors $\boldsymbol{x}$ and $\tilde{\boldsymbol{x}}$ are square law equivalent if and only if $\Upsilon(\boldsymbol{x}) = \Upsilon(\tilde{\boldsymbol{x}})$, and we denote the equivalence by $\boldsymbol{x} \equiv \tilde{\boldsymbol{x}}$.

System model
Class representative

Class representative

The Class representative block consist of a set $\mathcal{S}$ of cardinality M, whose elements belong to $\mathbb{C}^n$ and are all square law distinct, that is:

$$\mathcal{S} = \{\boldsymbol{x}_1, \ldots, \boldsymbol{x}_M\} \subset \mathbb{C}^n \qquad \text{such that} \qquad \boldsymbol{x}_i \not\equiv \boldsymbol{x}_l \Leftrightarrow k \neq l \tag{23}$$

and for an input $k \in \{1, \ldots, M\}$ the block outputs $\boldsymbol{x}_k$:

Equivalence class

Let us define equivalence class as the set of all vectors, that are equivalent, so an equivalence class $\mathcal{E}$ of size L is given by:

$$\mathcal{E} = \{\boldsymbol{x}_1, \ldots, \boldsymbol{x}_L\} \subset \mathcal{K}^n \qquad \text{such that} \qquad \boldsymbol{x}_i \equiv \boldsymbol{x}_j \quad \forall i, j \in \{1, \ldots, L\} \tag{24}$$

System model

Ambiguities

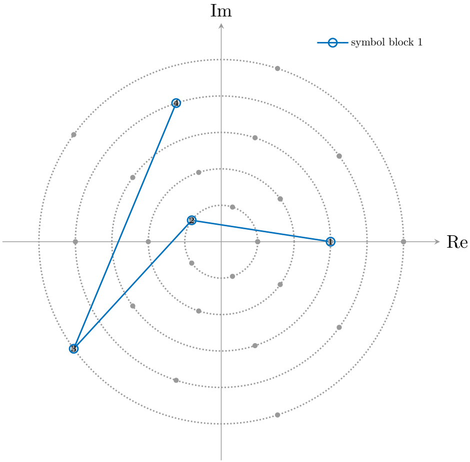

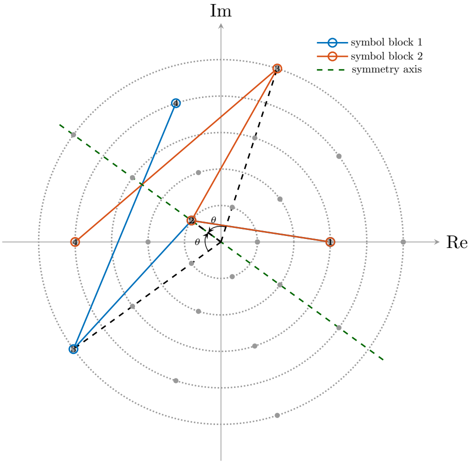

System model
Ambiguities

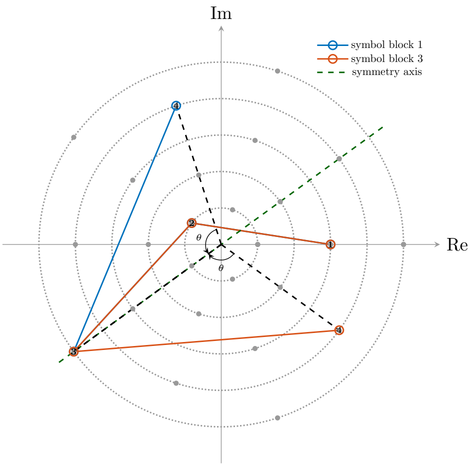

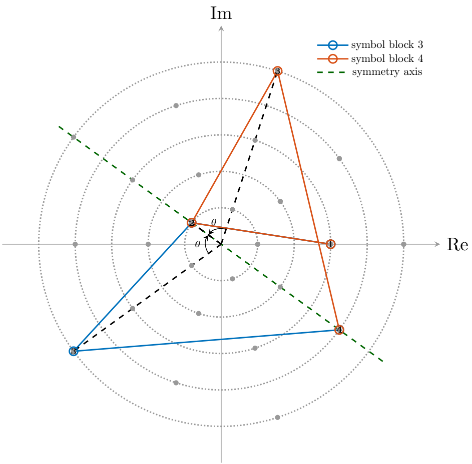

System model

Ambiguities

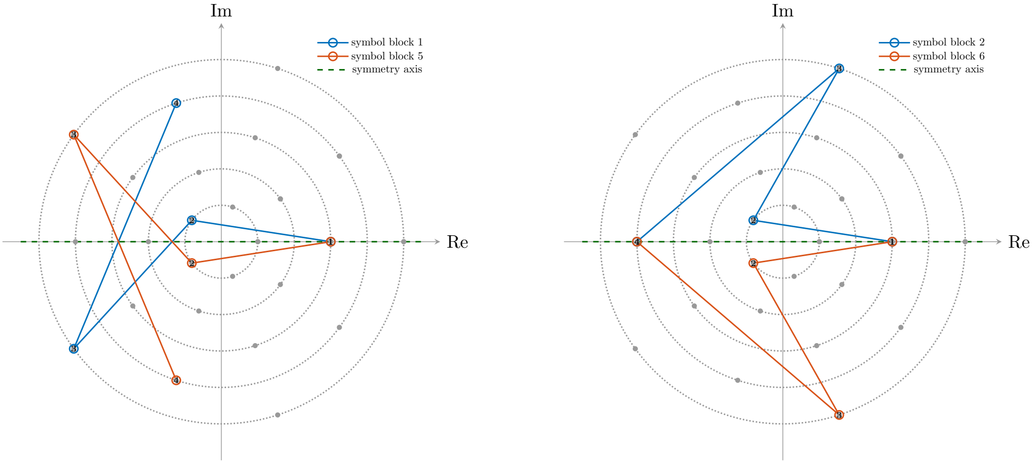

System model
Ambiguities

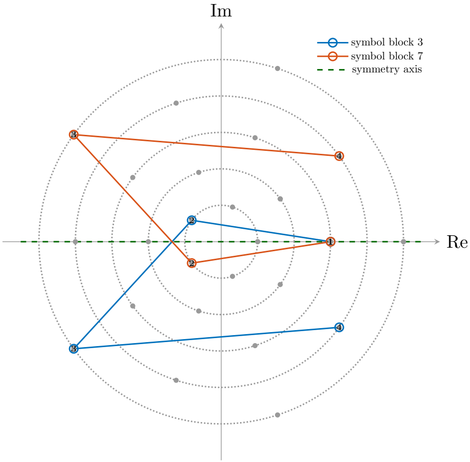

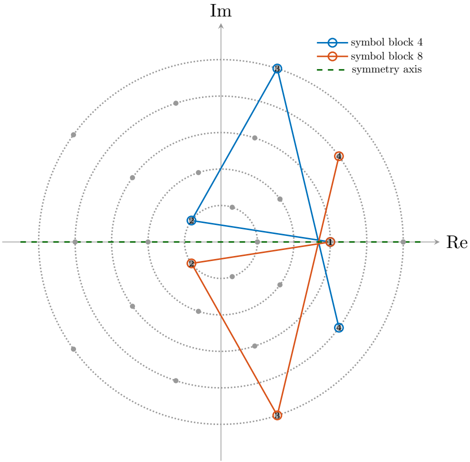

System model

Ambiguities

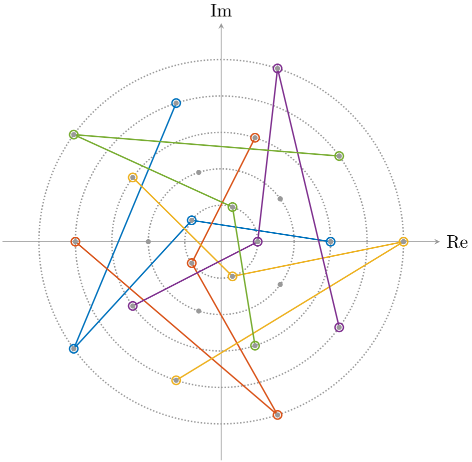

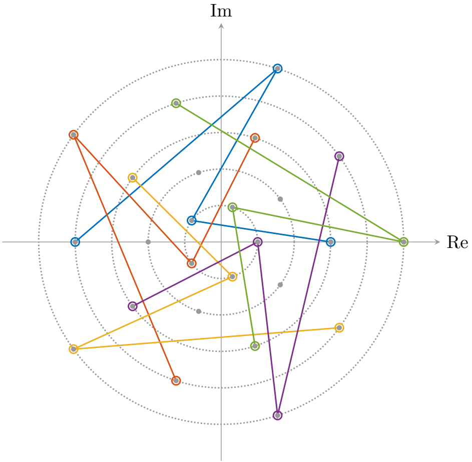

System model
Ambiguities

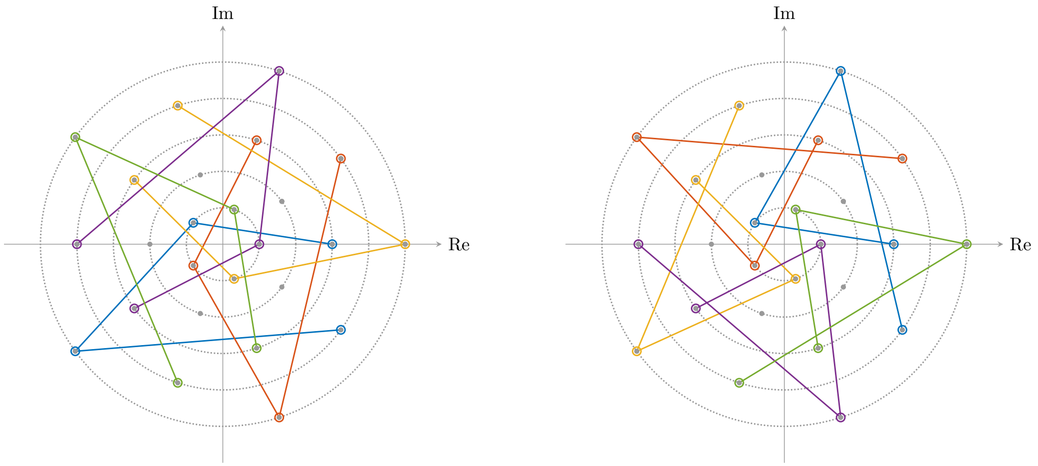

System model
Ambiguities

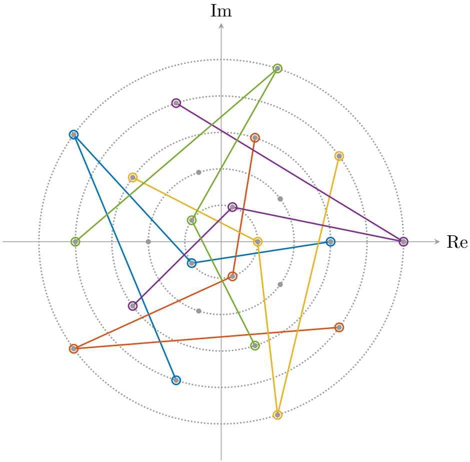

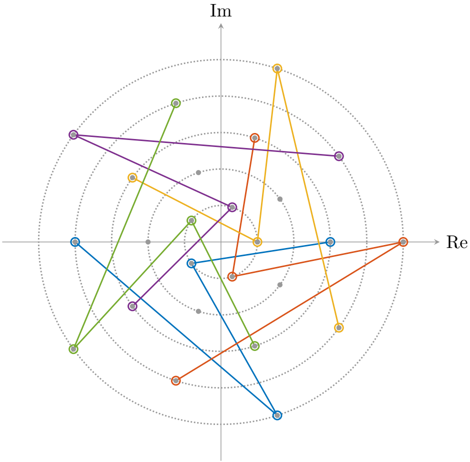

System model

Ambiguities

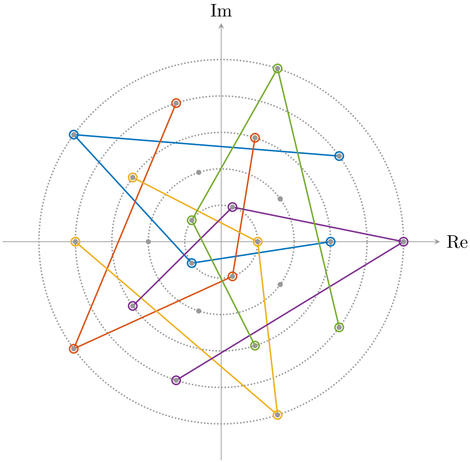

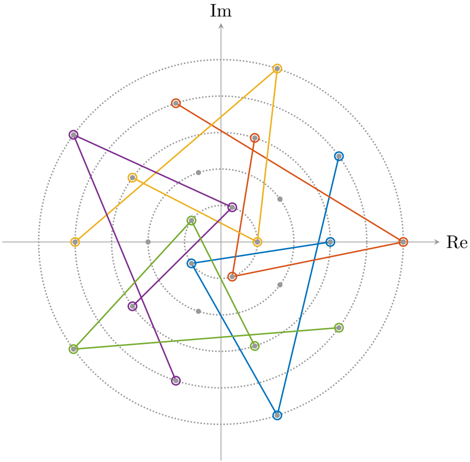

System model
Ambiguities

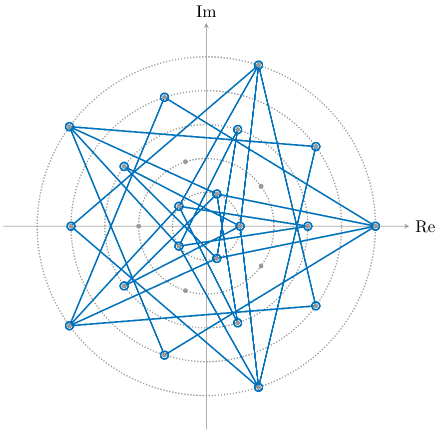

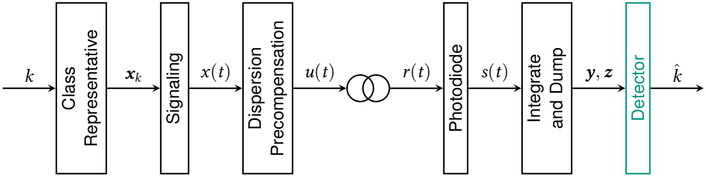

For the detection, the maximum-likelihood (ML) criterion is chosen:

$$\hat{k} = \underset{d \in \{1,\dots,M\}}{\arg\max}\ f\left(\boldsymbol{y}, \boldsymbol{z} | \boldsymbol{x}_d\right) \tag{25}$$

Where the PDF of $\boldsymbol{y}, \boldsymbol{z}$ given $\boldsymbol{x}_d$ is given by :

$$f\left(\boldsymbol{y}, \boldsymbol{z} | \boldsymbol{x}_d\right) = f\left(\boldsymbol{y} | \boldsymbol{x}_d\right) f\left(\boldsymbol{z} | \boldsymbol{x}_d\right) = \prod_{i=0}^{n-1} f\left(y_i | \boldsymbol{x}_d[i]\right) \prod_{i=0}^{n-2} f\left(z_i | \boldsymbol{x}_d[i], \boldsymbol{x}_d[i+1]\right) \tag{26}$$

Numerical simulation

Simulation for a 2-ring 4-ary constellation

Class size \ Block length	3	4	5	6	7
4	32	128	512	2048	8192
8	32	192	1024	5120	24576
16	8	96	768	5120	30720
32		16	256	2560	20480
64			32	640	7680
128				64	1536
256					128
Total	72	432	2592	15552	93312
Rate loss (bit/sym)	0.94	0.81	0.73	0.68	0.64

Table 1: Number of equivalence classes for 2-ring 4-ary Phase constellation.

Numerical simulation

Simulation for a 2-ring 4-ary constellation

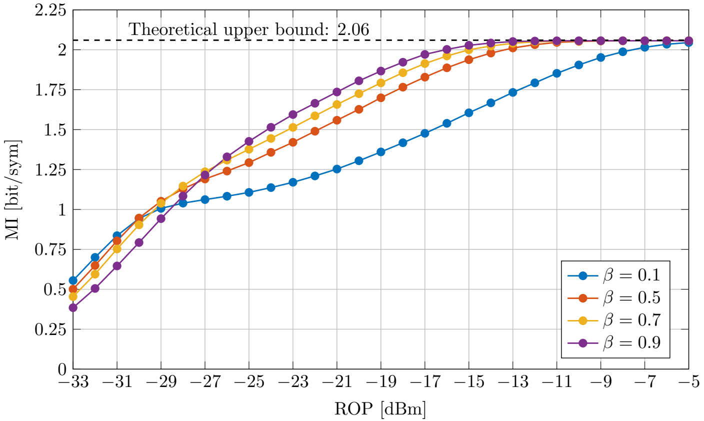

Figure 13: Mutual information of the system with 2-ring 4-ary phase constellation and symbol block length $n = 3$.

Numerical simulation

Simulation for a 2-ring 4-ary constellation

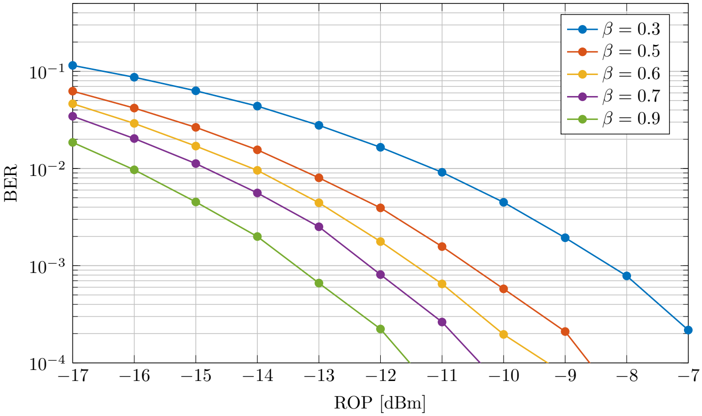

Figure 14: Bit error rate of the system with 2-ring 4-ary phase constellation and symbol block length $n = 4$.

Discussion

Karlsruhe Institute of Technology

Disadvantages

- **The complexity of the decoder**: To decrease the rate loss the block length must increase, but the complexity grows exponentially with the block length.
- **The bandwidth efficiency**: Tukey window is a time limited signal, hence its spectrum is wide, so the bandwidth efficiency is bad.
- **The implementation**: The integrate and dump block is an analog and hence may be difficult to implement.

Generalized direct detection with phase recovery

System model

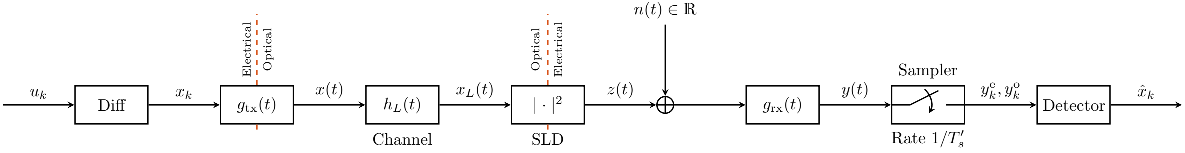

System model
Differential encoder

The phase encoding is done by a function that receives as an input a vector of symbols $\boldsymbol{u}$ and outputs a vector of symbols $\boldsymbol{x} = f_{\text{diff}}(\boldsymbol{u})$ with the same magnitude as the symbols in $\boldsymbol{u}$, and a given phase based on a set of conditions

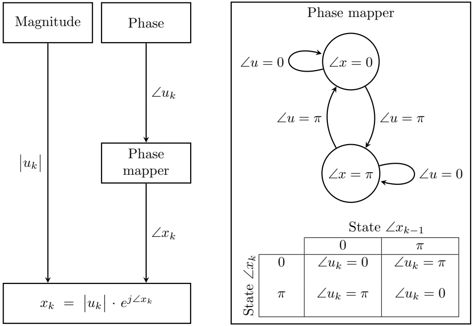

State $\angle x_k$ \ State $\angle x_{k-1}$	0	π
0	$\angle u_k = 0$	$\angle u_k = \pi$
π	$\angle u_k = \pi$	$\angle u_k = 0$

Figure 15: Differential phase mapper example for M-ASK.

System model
Transmitter

The transmitter receives as input a sequence $\boldsymbol{x} = \{x_0, \ldots, x_{n-1}\}$ of independent and identically distributed (i.i.d.) symbols x_i taken from a finite constellation $\mathcal{K} = \{a_1, \ldots, a_q\}$ with q elements, and outputs a signal given by:

$$x(t) = \sum_{k=0}^{n-1} x_k \cdot g_{\text{tx}}(t - iT) \tag{27}$$

where T is the inverse of the symbol rate, $x_i \in \mathcal{K}$, and $g_{\text{tx}}(t)$ is the pulse waveform.

System model
Transmission medium and receiver

The channel considered is an optic fiber that only presents chromatic dispersion, characterized in the frequency domain by:

$$H_L(f) = e^{j2\beta_2 L\pi^2 f^2} \tag{28}$$

where β_2 is the group-velocity dispersion parameter and L is the fiber length.
The receiver consists of a photodiode, whose output is given by:

$$z(t) = |x_L(t)|^2 \tag{29}$$

System model
sampler

For the sample an oversampling factor of $N_{\text{os}} = T_s / T_s' = 2$ is used. Let $\boldsymbol{x}' = \{0, x_0, \dots 0, x_{n-1}\}$ and $\boldsymbol{y}' = \{y_0, \dots, y_{2n-1}\}$ be the upsampled sequence at the transmitter and receiver.

$$y_k' = z_k' + n_k' \tag{30}$$

$$z_k' = \left(|x_L(t)|^2 * g_{\text{rx}}(t)\right)_{t=kT_s'} \tag{31}$$

where $n_k \sim \mathcal{N}(0, \sigma_N^2)$ and $\sigma_N^2 = N_0 B$.
Now let us define the combined impulse response as $\psi(t) = g_{\text{tx}}(t) * h_L(t)$ and the discrete version of it $\psi_k = \psi(kT_s')$, then:

$$x_L(kT_s') = \sum_{m=0}^{2n-1} \psi_m x_{k-m}' \tag{32}$$

System model
sampler

Finally, if the pulse shape is a sinc pulse, $|x_L(t)|^2 * g_{\text{rx}} = |x_L(t)|^2$, so:

$$z'_k = \left| \sum_{m=0}^{2n-1} \psi_m x'_{k-m} \right|^2 \tag{33}$$

Which can be expressed in vector matrix notation if we define the Toeplitz matrix $\boldsymbol{\Psi}$ and the channel state $\boldsymbol{s}'_0 = [0, x_{-\widetilde{M}}, 0, x_{1-\widetilde{M}}, \ldots, 0, x_{-1}]^T$ as:

$$\boldsymbol{y}' = \left| \boldsymbol{\Psi} \begin{bmatrix} \boldsymbol{s}'_0 \\ \boldsymbol{x}' \end{bmatrix} \right|^{\circ 2} + \boldsymbol{n}' = \left| \boldsymbol{\Psi} \tilde{\boldsymbol{x}}' \right|^{\circ 2} + \boldsymbol{n}' \qquad \in \mathbb{R}^{2n} \tag{34}$$

System model
Even and odd samples

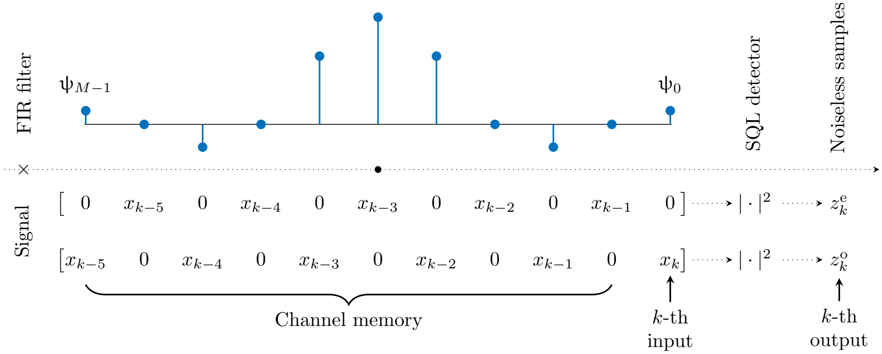

$$\boldsymbol{z}_k = \left[z'_{2k}, z'_{2k+1}\right] = \left[z_k^{\mathrm{e}}, z_k^{\mathrm{o}}\right] \qquad \boldsymbol{y}_k = \left[y_k^{\mathrm{e}}, y_k^{\mathrm{o}}\right] = \boldsymbol{z}_k + \left[n_k^{\mathrm{e}}, n_k^{\mathrm{o}}\right] \tag{35}$$

System model

Symbol-wise MAP detection

$$\hat{x}_k = \arg\max_{x_k} p(x_k, \boldsymbol{y}') p(x_k, \boldsymbol{y}') = \sum_{s_0} \sum_{\boldsymbol{x} \backslash x_k} p(s_0, \boldsymbol{x}, \boldsymbol{y}') \tag{36}$$

and $\sum_{\boldsymbol{x} \backslash x_k}$ denotes a sum over all possible vectors $\boldsymbol{x}$ but where the k-th position is fixed.

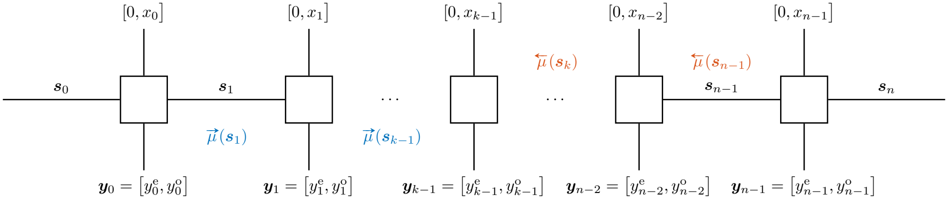

Numerical simulation
Auxiliary channel

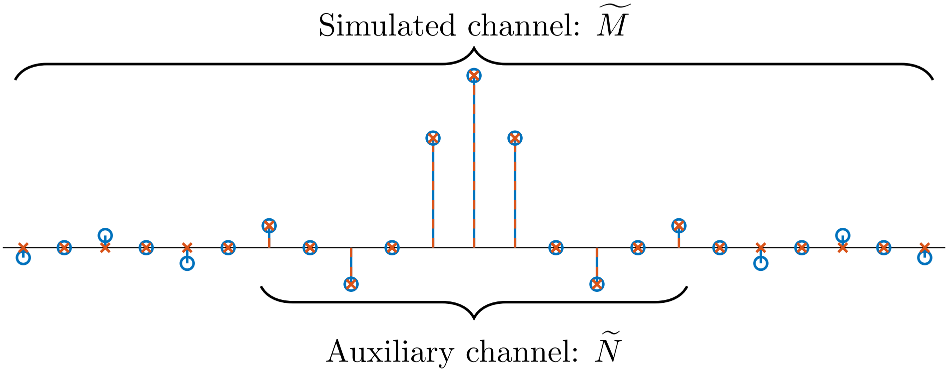

Numerical simulation
Constellations

For the simulation we used BPSK, QAM, and a specially designe constellation, named DD-SQAM.

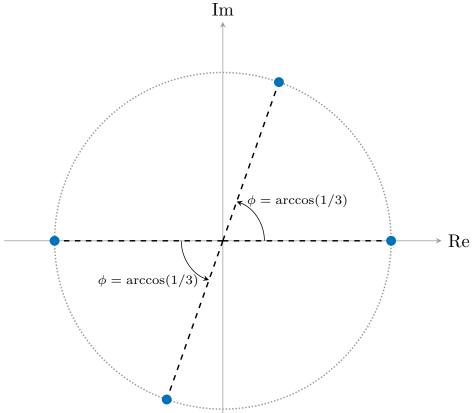

Numerical simulation

Results

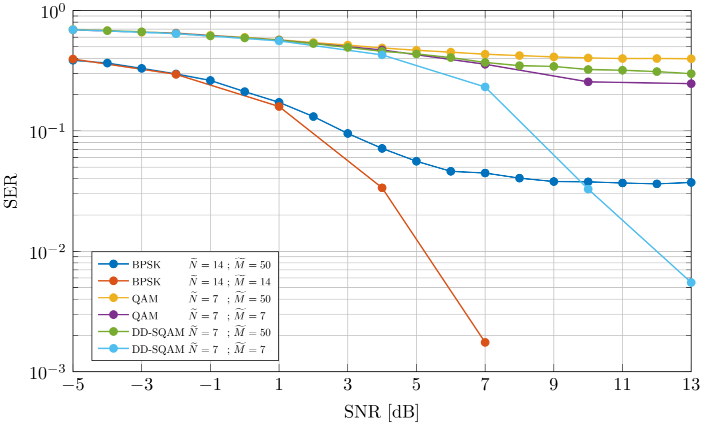

Discussion

- The system is more flexible, since the waveform have no restriction.
- The spectral efficiency is better than in the previous system.
- The system has an oversampling of only 2.
- The decoder is still to complex to be feasible.

MagPhase-DetNet

Architecture

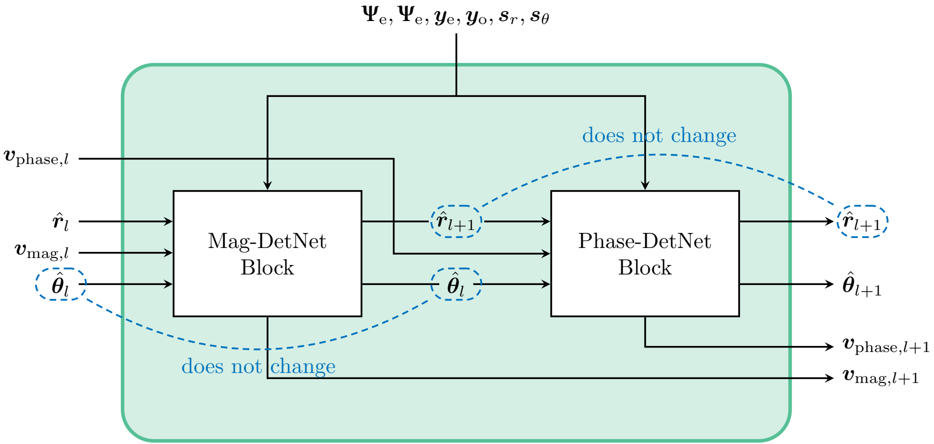

Architecture

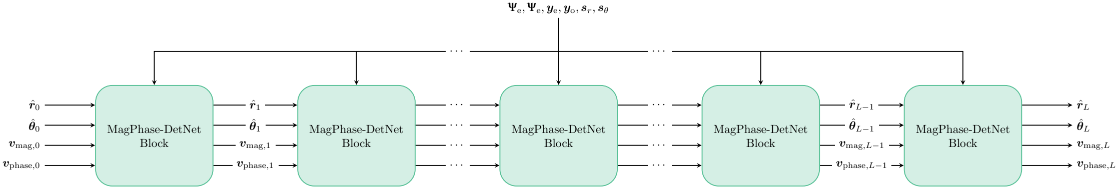

Numerical simulation

Training process

For the training we use a variable batch size that takes the following values in order $[100, 400, 1000, 2000, 5000, 10000]$ and performs 300 learning processes for each batch size.

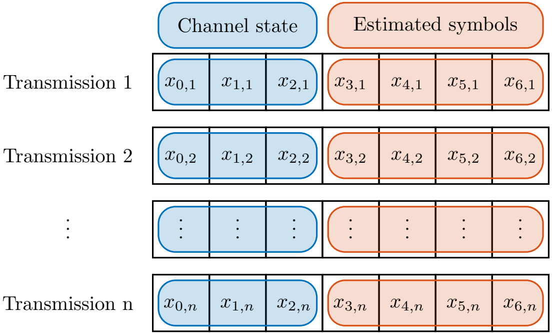

Numerical simulation
Evaluation process

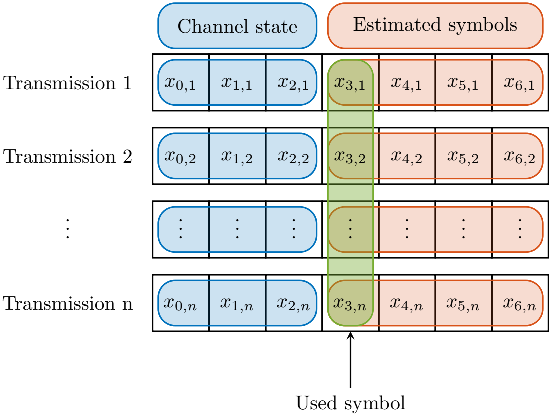

Numerical simulation
Evaluation process

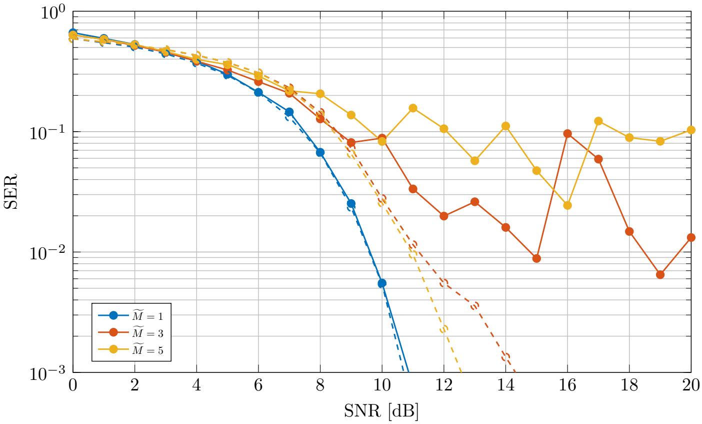

Numerical simulation
Evaluation process

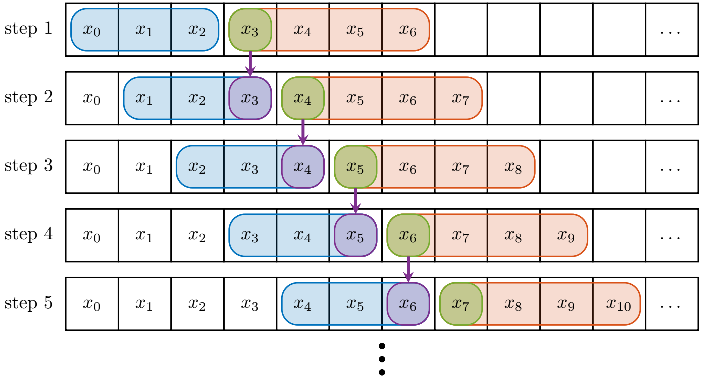

Numerical simulation

Evaluation process

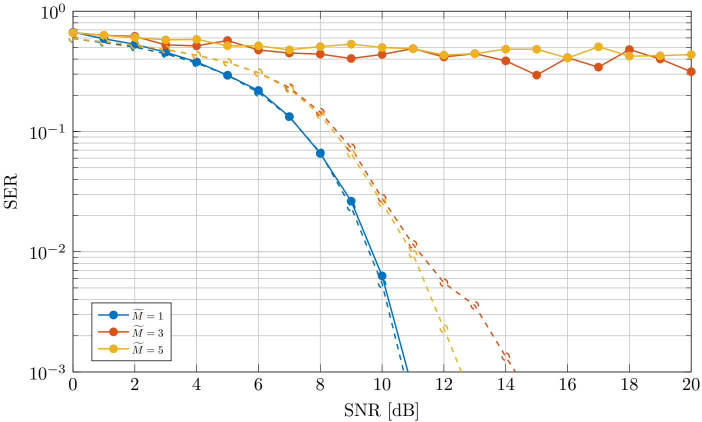

Conclussions

- The trained MagPhase-DetNet network's performance is not as good as needed because the trained models present a high error floor.
- When trying the sequential evaluation the bad performance shows that the architecture is not the most adequate, may be a conventional approach could be better.
- The training process seems to be slower for longer channel memory.

References I

[1] Govind P. Agrawal. "Introduction". In: *Fiber-Optic Communication Systems*. John Wiley & Sons, Ltd, 2010. Chap. 1, pp. 1–23. ISBN: 9780470918524. DOI: `https://doi.org/10.1002/9780470918524.ch1`. eprint: `https://onlinelibrary.wiley.com/doi/pdf/10.1002/9780470918524.ch1`. URL: `https://onlinelibrary.wiley.com/doi/abs/10.1002/9780470918524.ch1`.

[2] Govind P. Agrawal. "Optical Receivers". In: *Fiber-Optic Communication Systems*. John Wiley & Sons, Ltd, 2010. Chap. 4, pp. 128–181. ISBN: 9780470918524. DOI: `https://doi.org/10.1002/9780470918524.ch4`. eprint: `https://onlinelibrary.wiley.com/doi/pdf/10.1002/9780470918524.ch4`. URL: `https://onlinelibrary.wiley.com/doi/abs/10.1002/9780470918524.ch4`.

[3] David J. C. MacKay. *Information theory, inference, and learning algorithms*. 15th print. Cambridge [u.a.]: Cambridge University Press, 2015. ISBN: 9780521642989. URL: `http://bvbr.bib-bvb.de:8991/F?func=service&doc_library=BVB01&doc_number=020774035&line_number=0001&func_code=DB_RECORDS&service_type=MEDIA`.

References II

[4] Antonio Mecozzi and Mark Shtaif. “Information Capacity of Direct Detection Optical Transmission Systems”. In: *Journal of Lightwave Technology* 36.3 (2018), pp. 689–694. DOI: 10.1109/JLT.2017.2777188.

[5] Daniel Plabst et al. “Achievable Rates for Short-Reach Fiber-Optic Channels With Direct Detection”. In: *Journal of Lightwave Technology* 40.12 (2022), pp. 3602–3613. DOI: 10.1109/JLT.2022.3149574.

[6] Tobias Prinz et al. *Successive Interference Cancellation for Bandlimited Channels with Direct Detection*. 2023. arXiv: 2212.07761 [cs.IT].

[7] Neev Samuel, Tzvi Diskin, and Ami Wiesel. “Deep MIMO detection”. In: *2017 IEEE 18th International Workshop on Signal Processing Advances in Wireless Communications (SPAWC)*. 2017, pp. 1–5. DOI: 10.1109/SPAWC.2017.8227772.

[8] Neev Samuel, Tzvi Diskin, and Ami Wiesel. “Learning to Detect”. In: *IEEE Transactions on Signal Processing* 67.10 (2019), pp. 2554–2564. DOI: 10.1109/TSP.2019.2899805.

References III

[9] Marco Secondini and Enrico Forestieri. “Direct Detection of Bipolar Pulse Amplitude Modulation”. In: *Journal of Lightwave Technology* 38.21 (2020), pp. 5981–5990. DOI: 10.1109/JLT.2020.3007584.

[10] Amir Tasbihi and Frank R. Kschischang. “Direct Detection Under Tukey Signalling”. In: *Journal of Lightwave Technology* 39.21 (2021), pp. 6845–6857. DOI: 10.1109/JLT.2021.3109852.

[11] Amir Tasbihi and Frank R. Kschischang. “On the Capacity of Waveform Channels Under Square-Law Detection of Time-Limited Signals”. In: *IEEE Transactions on Information Theory* 66.11 (2020), pp. 6682–6687. DOI: 10.1109/TIT.2020.2999889.

[12] Taotao Wang et al. “Joint Multiple Symbol Differential Detection and Channel Decoding for Noncoherent UWB Impulse Radio by Belief Propagation”. In: *IEEE Transactions on Wireless Communications* 16.1 (2017), pp. 293–306. DOI: 10.1109/TWC.2016.2623301.